

## Effects of Bundle/Hole Coupling Parameters in the Two-Fluid Thermal-Hydraulic Analysis of Quench Propagation in Two-Channel Cable-In-Conduit Conductors

Roberto Zanino, Laura Savoldi and Federica Tessarin  
Dipartimento di Energetica, Politecnico, I-10129 Torino, Italy

Luca Bottura  
CERN, Div. LHC-MTA, CH-1211 Geneve 23, Switzerland

**Abstract**— Thermal-hydraulic modeling of cable-in-conduit conductors (CICC) with a two-channel bundle/hole (B/H) topology contains several uncertainties in the B/H coupling model. Here we study numerically with the 2-fluid MITHRANDIR code some effects of the major coupling parameters, i.e., degree of perforation of the B/H interface and heat transfer coefficient through it, on quench propagation in a two-channel CICC. A semi-quantitative discussion of the results is presented.

### I. INTRODUCTION

The International Thermonuclear Experimental Reactor (ITER) will use cable-in-conduit conductors (CICC), with a two-channel topology. The cables are wound in an annular region (bundle  $\equiv$  B) around a central channel (hole  $\equiv$  H), which provides pressure exhaust in case of a quench and lower impedance for the supercritical helium coolant.

The MITHRANDIR code, specifically developed [1] for the analysis of thermal-hydraulic transients in two-channel CICC, implements a two-fluid model allowing for different flow and thermodynamic state of the helium in the B&H regions. This detail proved to be essential in the validation against data from the Quench Experiment on Long Length (QUELL) [2], where the 2-fluid description showed a much better accuracy than the traditional 1-fluid assumption of same pressure and temperature in the two regions [3], [4].

However, several uncertainties are present in the B/H coupling model in the form of "free" parameters, which can hardly be determined experimentally, clearly showing the need for parametric studies. (A coupling model alternative to the simplified one used in MITHRANDIR was presented very recently [5]).

Here we study some qualitative effects of the major coupling parameters on quench propagation in two-channel CICC. This study is also motivated by previous work [4] where quench acceleration  $\sim 0.5$ - $1.0$  m/s<sup>2</sup> was computed for QUELL by the 2-fluid model and observed in the experiment, while the 1-fluid model predicted a decelerating quench ( $\sim -0.4$  m/s<sup>2</sup>) [4]. Significant effects of B/H coupling parameters on the stability margin were computed for ITER conductors [6], and for QUELL [7], but they will be discussed elsewhere.

Manuscript received September 14, 1998.

The work at Politecnico di Torino was partially financially supported by Euratom under contract NET/96-424.

### II. BUNDLE/HOLE COUPLING PARAMETERS IN THE TWO-FLUID MITHRANDIR MODEL

In the MITHRANDIR model [1] the helium in the bundle and the helium in the hole can exchange mass, momentum and energy through the perforated interface.

The actual perforated fraction  $F$  is the first B/H coupling parameter considered here.  $F$  is generally unknown and typically lower than its nominal value, because the cables can partially obstruct the holes/passages left open in the interface design. The mass exchange through the perforation is assumed to be  $\propto F \times \sqrt{p_B - p_H}$ .

The other major B/H coupling parameter is the effective heat transfer coefficient between B and H

$$h_{\text{eff}} = F H_{\text{NW}} h_{\text{nowall}} + (1 - F) H_{\text{W}} h_{\text{wall}} \quad (1)$$

where the steady state contributions to the local heat transfer coefficients  $h_{\text{wall}}$  and  $h_{\text{nowall}}$  are based mainly on experimental correlations, which depend on the Reynolds number  $Re$  [1]. Here two artificial multipliers,  $H_{\text{NW}}$  and  $H_{\text{W}}$ , are used for the parametric treatment of conduction through perforation and wall respectively. The conductive portion of the heat exchange between B and H is assumed to be  $\propto h_{\text{eff}} \times (T_B - T_H)$ . Note that mass exchange through the perforation gives also a convective contribution to the heat flux.

### III. TEST CASE

We shall consider in the following a conductor with geometrical data as in QUELL [2], except  $X_{\text{LENGT}}=40$ m. The pressure difference  $\Delta p_0$  between inlet and outlet is varied parametrically.

The transport current is constant at 8kA and the magnetic field is 11T and uniform. Initial operating conditions are linear pressure profile with average  $p_0=6$ bar, constant temperature  $T_0=6.9$ K. The current sharing temperature is  $T_{cs}=9.4$ K.

The quench is initiated by an external heating pulse (EHP). Only the jacket is directly heated by the EHP, which is centered along the conductor at  $x=20$ m. The EHP lasts for  $\tau_0=0.2$ s and extends over a length  $IHZ=1$ m. The input power per unit conductor length is  $Q_0=2$  kW/m.

The independence of the solutions obtained on mesh and time step was checked numerically.

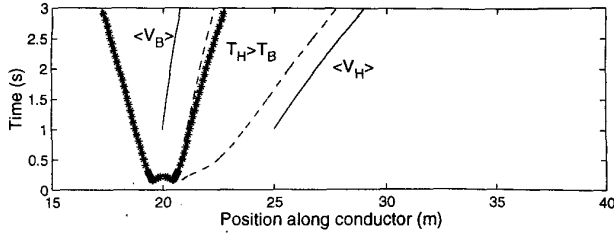


Fig. 1. Evolution of quench front (\*) and of  $T_H=T_B$  front (dashed). Reference slopes of helium flow speed in bundle  $\langle V_B \rangle$  and in hole  $\langle V_H \rangle$  at the right quench front (solid lines). Case  $\Delta p_0=0\text{bar}$ ,  $F=0.01$ ,  $H_w=0$ ,  $H_{NW}=10$ .

#### IV. EFFECTS ON QUENCH PROPAGATION

##### A. Quench Speed

Let us consider in Fig. 1 a typical case with initially stagnant helium ( $\Delta p_0=0$ ). The quench propagates symmetrically with respect to the center of the conductor, with a speed  $V_q \geq \langle V_B \rangle$ , the average flow speed of the bundle helium at the quench front. In the initial transient the presence of 2 normal zones (i.e., 4 normal fronts) under the IHZ gives a fast increase of the normal zone (NZ) in time. Afterwards  $V_q$  is approximately constant, i.e., no significant quench acceleration appears within the "observation" time of 3s from the beginning of the EHP.

Let us now consider in Fig. 2a the effects of purely hydraulic B/H coupling ( $H_w = H_{NW} = 0$ ) on  $V_q$ , by varying the perforation  $F$ . In the case  $F=0$  it turns out that  $V_q \sim V_B$ .  $V_B$  can be estimated from the approximate momentum balance for B helium (see [1] for definitions)

$$-\partial p_B / \partial x \sim 2(p_B^{\max} - p_0) / X_{\text{LENGT}} \sim 2f_B \rho V_B^2 / D_B. \quad (2)$$

TABLE I  
CONVECTIVE BUNDLE → HOLE ENERGY TRANSPORT AT QUENCH FRONT

$H_{NW}$	F=0.001		F=0.01		F=0.1		F=0.99	
	$\Delta p/p$	Flux	$\Delta p/p$	Flux	$\Delta p/p$	Flux	$\Delta p/p$	Flux
0.	2.e-3	7.e1	4.e-5	1.e2	5.e-7	1.e2	5.e-9	1.e2
1.e0	2.e-3	7.e1	4.e-5	1.e2	4.e-7	2.e2	5.e-9	2.e2
1.e2	2.e-3	7.e1	5.e-5	2.e2	1.e-6	3.e2	1.e-8	3.e2
1.e4	2.e-3	1.e2	1.e-4	3.e2	1.e-6	3.e2	1.e-8	3.e2

$\Delta p_0=0$ ,  $H_w = 0$ . Maximum of  $(p_B - p_H)/p_B$  over the whole transient, and time averaged convective heat flux (W/m) from bundle to hole in the temperature equation [1].

TABLE II  
CONDUCTIVE BUNDLE → HOLE ENERGY TRANSPORT AT QUENCH FRONT

$H_{NW}$	F=0.001		F=0.01		F=0.1		F=0.99	
	$\Delta T/T$	Flux	$\Delta T/T$	Flux	$\Delta T/T$	Flux	$\Delta T/T$	Flux
0.	-1.e0	0	-6.e-1	0	-6.e-1	0	-6.e-1	0
1.e0	-1.e0	-2.e-1	-6.e-1	-1.e0	-6.e-1	-1.e2	-2.e-1	-1.e2
1.e2	-7.e-1	-2.e1	-2.e-1	-1.e2	-3.e-2	-4.e2	-4.e-3	-4.e2
1.e4	-4.e-2	-4.e2	-4.e-3	-4.e2	-4.e-4	-4.e2	-4.e-5	-4.e2

$\Delta p_0=0$ ,  $H_w = 0$ . Maximum of  $(T_B - T_H)/T_B$  over the whole transient, and time averaged conductive heat flux (W/m) from bundle to hole in the temperature equation [1].

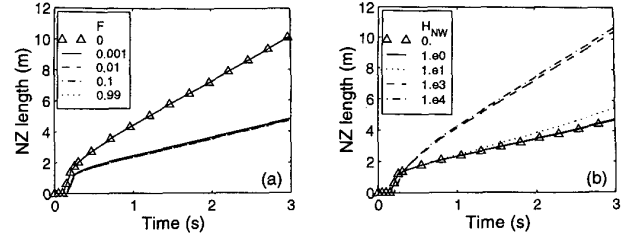


Fig. 2. Case  $\Delta p_0=0\text{bar}$ ,  $H_w=0$ . (a) Effect of perforation  $F$  with  $H_{NW}=0$ . (b) Effect of heat conduction through perforation with  $F=0.01$ .

From (2) one finds  $V_q \sim 1\text{m/s}$ , in good agreement with Fig. 2a. For any finite  $F$ ,  $V_q$  is approximately the same and it is much smaller (about 1/3, for the case at hand) than if  $F=0$ . The latter effect is due to the pressure relief in the bundle provided by the perforation [ $p_B^{\max}(x=20\text{m})$  is  $\sim 8.9\text{bar}$  for  $F=0$  and  $\sim 6.8\text{bar}$  for  $F \neq 0$ ]. Since the friction factor  $f_B$  scales roughly as  $1/V_B$  at  $Re_B \sim 100$ , (2) leads to a reduction of  $V_B$  (and  $V_q$ ) by a factor  $2.9/0.8 \approx 3$ , in good agreement with Fig. 2a. Any finite  $F$  gives similar  $V_q$  because the driving  $p_B$  is more or less the same. Also,  $p_B - p_H$  decreases for increasing  $F$  in a way such that the convective B/H heat flux stays approximately constant see Table I and the discussion of Fig. 2b below.

If we "turn on" conduction between B and H with  $F=0$  (not shown), then  $V_q$  is approximately independent of  $H_w$  because  $p_B$  does not vary significantly when  $H_w$  increases from 0 to, say, 100. In Fig. 2b conduction between B and H is turned on for a given finite value of  $F=0.01$ .  $V_q$  increases with  $H_{NW}$  because the B/H thermal coupling becomes more effective as  $H_{NW}$  is increased. Indeed, for small  $F$  the increase in  $H_{NW}$  leads to a weaker decrease of  $|T_B - T_H|$  so that the conductive B/H heat flux increases, until it saturates for large  $H_{NW}$ , see Table II. The faster helium in the hole, together with the increasing coupling, drives a faster quench, with a limiting speed  $\sim (V_B A_B + V_H A_H) / (A_B + A_H)$  in the case of perfect coupling. Notice finally that the convective contribution to the B/H heat flux at the quench front is *not* negligible compared to the conductive one (see Tables I, II).

##### B. Quench Acceleration

When the initial pressure drop  $\Delta p_0 \neq 0$  over the conductor,

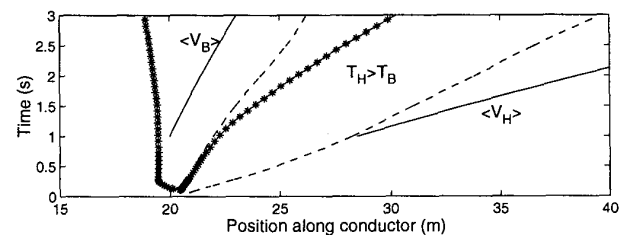


Fig. 3. Evolution of quench front (\*) and of  $T_H=T_B$  front (dashed). Reference slopes of helium flow speed in bundle  $\langle V_B \rangle$  and in hole  $\langle V_H \rangle$  at the right quench front (solid lines). Case  $\Delta p_0=3\text{bar}$ ,  $F=0.01$ ,  $H_w=0$ ,  $H_{NW}=10$ .

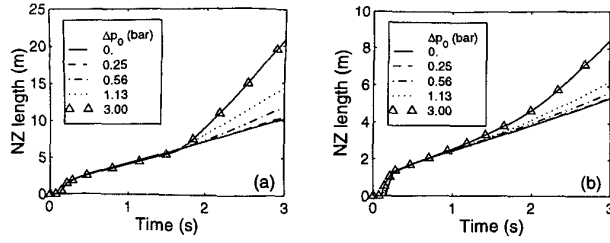


Fig. 4. Effect of  $\Delta p_0$  with  $H_w=1$ . (a) Case  $F=0$ . (b) Case  $F=0.01$ ,  $H_{NW}=0$ .

noticeable quench acceleration  $a_q \equiv dV_q/dt > 0$  is observed as shown in Fig. 3. If we concentrate on the right quench front, we notice that initially  $V_q \sim <V_B>$ , then the quench starts accelerating as the front enters the  $T_H > T_B$  region. This behavior can be qualitatively explained (see also next Section) in terms of preheating, i.e., of entrainment of the temperature front of the slower B helium (and consequently of the quench) by the faster H helium.

In the presence of B/H thermal coupling  $a_q$  increases for increasing  $\Delta p_0$  as shown in Fig. 4a and Fig. 4b, for the non perforated and perforated case respectively, while in the case of vanishing B/H coupling (not shown)  $a_q \approx 0$  for any  $\Delta p_0$ . (Notice that “large”  $\Delta p_0$ , although useful to emphasize parametric dependencies, can unnecessarily involve helium compressibility effects).

A large  $\Delta p_0$  gives rise to a large initial  $V_H$  and therefore a large  $h_{wall}$ . In the case of Fig.4a ( $F=0$ ) this gives a fast increase of  $p_H$  because of heating from the bundle. In the case of Fig.4b ( $F \neq 0$ )  $p_B \sim p_H$  and the stronger increase of  $p_H$  for larger  $\Delta p_0$  is due to a stronger increase of  $p_B$ , which is due in turn to better coupling between B helium and conductor. In any case,  $V_H$  will further nonlinearly increase. This qualitatively leads to effective preheating of the B helium ahead of the quench front, i.e., to stronger acceleration of the quench (see below).

Tests with increasing  $h_{eff}$  give a nonmonotonic behavior of  $a_q$  as in Fig. 5a and Fig. 5b, for the nonperforated and perforated case respectively. In the case of Fig. 5a for both “too small” and “too large”  $H_w$  the hole cannot, for different reasons (see below), significantly preheat the bundle. In Fig. 5b the situation is similar. For small  $H_{NW}$  the acceleration increases, because the preheating flux increases with  $H_{NW}$ .

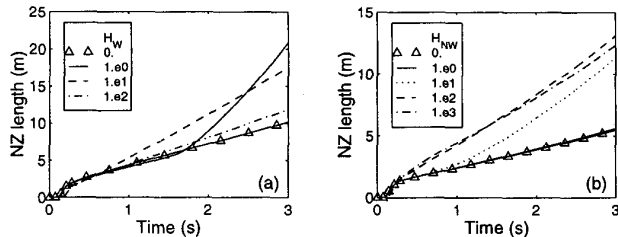


Fig. 5. Effect of B/H heat conduction with  $\Delta p_0=3$ bar. (a) Case  $F=0$ . (b) Case  $F=0.01$ ,  $H_w=0$ .

Then, for even larger  $H_{NW}$ ,  $V_q$  tends to become constant in time, because  $T_B \sim T_H$ , and no preheating is possible. The “GANDALF equivalent” case with  $H_{NW}=1.e4$  and  $F=0.99$  behaves essentially as the case with  $H_{NW}=1.e3$  and  $F=0.01$ .

### C. Qualitative analysis of quench acceleration

Let us consider in a bit more detail the issue of B helium preheating by the faster H helium, and its influence on quench acceleration.

Figs. 6 and 7 refer to cases with  $H_w=1$  and  $H_w=10$  respectively, taken from Fig. 5a. It is clear that one does not have acceleration unless (as in Fig. 6) both following conditions are satisfied ahead of the front: 1) sufficiently large heat flux from H to B and 2) sufficiently hotter helium in H than in B (not satisfied in Fig. 7). This is a fairly general conclusion which applies also (not shown) when comparing the cases with  $H_{NW}=10$  and 100 from Fig. 5b.

The preheating, however, will be effective roughly speaking only if B/H heat exchange is faster than convection in the bundle. The B/H (conductive) heat exchange time scale can be defined as

$$\tau_{BH} = [h_{eff}P(1/\rho_B C_{vB} A_B + 1/\rho_H C_{vH} A_H)]^{-1} \quad (3)$$

where the wetted perimeter  $P=2\sqrt{\pi A_H}$ . If  $\delta(t)$  is the distance between the temperature fronts ( $T=T_{cs}$ , say) in H and B, the mentioned condition for preheating reads  $\tau_{BH} < \delta/V_B^T$ , where  $V_B^T(t)$  is the propagation speed of the  $T_B$  front. This relation is indeed verified in all cases which show noticeable acceleration here, while cases with  $a_q \approx 0$  satisfy  $\tau_{BH} > \delta/V_B^T$ .

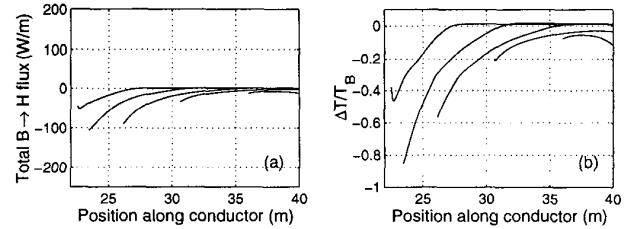


Fig. 6. Spatial profiles ahead of instantaneous right quench front position at  $t=1, 1.5, 2, 2.5, 3$  s. Case  $\Delta p_0=3$ bar,  $F=0$ ,  $H_w=1$ . (a) Total heat flux (W/m) from B to H, in the temperature equation [1]. (b)  $(T_B-T_H)/T_B$ .

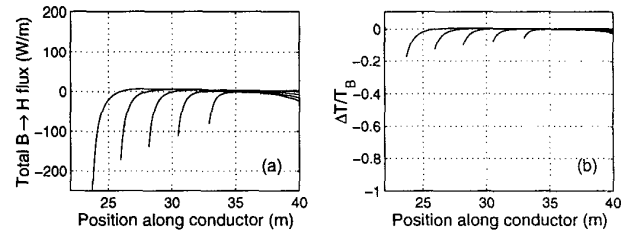


Fig. 7. Spatial profiles ahead of instantaneous right quench front position at  $t=1, 1.5, 2, 2.5, 3$  s. Case  $\Delta p_0=3$ bar,  $F=0$ ,  $H_w=10$ . (a) Total heat flux (W/m) from B to H, in the temperature equation [1]. (b)  $(T_B-T_H)/T_B$ .

Under several simplifying assumptions Freidberg and Shaji have shown that (see [2] pp.128-130) the combination of radial shear between B and H of the axial helium flow speeds + radial conductive B/H heat transfer, results in an equivalent thermal diffusivity

$$\alpha = [A_B^2 A_H^2 / (A_B + A_H)^3] (\rho C / h_{eff} P) (V_B - V_H)^2 \quad (4)$$

along the conductor. (Small  $(T_B - T_H) / (T_B + T_H)$  was assumed in the derivation of (4), as a basis for time scale separation, which is not strictly verified here). From  $\alpha$  one can derive under further simplifying assumptions [8] an expression for the "additional" quench speed

$$V_{ad} = \sqrt{[Q\alpha / (T_{cs} - T_0)]} \quad (5)$$

where  $Q \sim \partial T / \partial t$ . A theoretical quench acceleration can then be computed, which is proportional to  $V_{ad}$  [8].

Without attempting a quantitative comparison, since not all of the above mentioned simplifying assumptions are satisfied in the case at hand, we can still correlate  $\alpha$  and  $V_{ad}$  with  $a_q$ , as in Table III. It appears that in the case of Figs. 6, 7, i.e., of Fig. 5a, the model qualitatively agrees with the numerical experiment, with larger  $\alpha$  and  $V_{ad}$  corresponding to larger  $a_q$ . The same model can qualitatively explain the correspondence between  $\Delta p_0$  and  $a_q$ . At large  $\Delta p_0$  the shear in the flow speeds increases, and the quadratic V dependence dominates in (4) over the linear one of  $h_{eff}$ .

The major discrepancy in the last row of Table III (small  $a_q$  with large  $\alpha$ ,  $V_{ad}$ ) can be easily explained considering Fig. 8. We notice that in this case a positive heat flux from B to H arises ahead of the quench front, so that no preheating and therefore no acceleration are possible, notwithstanding the negative temperature difference (hotter H). This implies that the heat flux between B and H is being dominated by convection, but this is not included in the simplified model of Freidberg and Shaji, which is therefore irrelevant in this case. The other smaller discrepancy in the fifth row of Table III can be explained similarly.

TABLE III  
COMPUTED AND ANALYTICAL MEASURES OF QUENCH ACCELERATION

Fig.	$\Delta p_0$ (bar)	F	$H_{NW}$	$H_w$	$a_q$ (m/s <sup>2</sup> )	$\alpha$ (m <sup>2</sup> /s)	$V_{ad}$ (m/s)
5a, 6	3	0.		1.	3.6	8.3	6.5
5a, 7	=	0.		10.	0.4	0.5	1.4
4b	=	0.01	0.	1.	1.5	6.2	6.6
	0	0.		1.	0.1	0.1	0.5
2b	=	0.01	0.	1.	0.1	0.5	2.0
5b	3	0.01	100.	=	0.6	0.2	1.1
3, 5b	=	=	10.	0.	0.9	2.6	4.0
5b, 8	=	=	1.	=	0.1	16.6	9.8

$a_q$  estimated by time derivation of quadratic least squares fit of right quench front evolution, for  $1s < t < 3s$ , except in first row for  $1.65s < t < 3s$ .

$\alpha$  from (4) and  $V_{ad}$  from (5), averaged values for  $1s < t < 3s$ .

$\alpha$  can be compared with Cu thermal diffusivity  $\alpha_{Cu} = 0.56 \text{ m}^2/\text{s}$ .

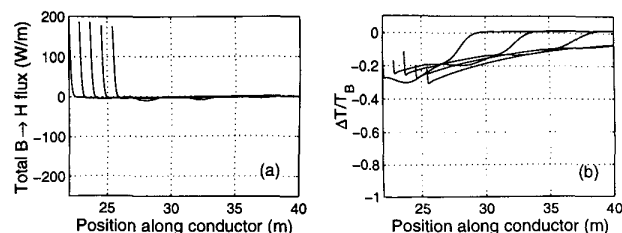


Fig. 8. Spatial profiles ahead of instantaneous right quench front position at  $t=1, 1.5, 2, 2.5, 3$  s. Case  $\Delta p_0=3$ bar,  $F=0.01$ ,  $H_{NW}=1$ ,  $H_w=0$ . (a) Total heat flux (W/m) from B to H, in the temperature equation [1]. (b)  $(T_B - T_H) / T_B$ .

## V. CONCLUSIONS AND PERSPECTIVE

Results of two-fluid quench modeling in two-channel CICC have been shown to depend on the assumptions made at the B/H coupling interface, and qualitative explanations of the parametric behavior have been presented.

In the QUELL-like conductor considered here the quench speed can vary by a factor of up to 3 for varying interface perforation F and/or B/H heat transfer coefficient  $h_{eff}$ .

Quench acceleration, as seen in the simulations here and in experiments in the past [2], is related to preheating of the slower B helium by the faster H helium. As such, it cannot be reproduced by one-fluid models assuming the same thermodynamic state for the helium in B and H.

In perspective we plan to develop a more quantitative theory of quench propagation in two-channel CICC and to extend the present analysis to the thermal-hydraulic stability problem [6], [7].

## REFERENCES

- [1] R. Zanino, S. DePalo, and L. Bottura, "A two-fluid code for the thermohydraulic transient analysis of CICC superconducting magnets", *J. Fus. Energy*, vol. 14, pp. 25-40, 1995.
- [2] A. Anghel, B. Blau, A. M. Fuchs, *et al.*, "The quench experiment on long length", Final Report, 1997.
- [3] R. Zanino, L. Bottura, and C. Marinucci, "A comparison between 1- and 2-fluid simulations of the QUELL conductor", *IEEE Trans. Appl. Supercond.*, vol. 7, pp. 493-496, 1997.
- [4] R. Zanino, L. Bottura, and C. Marinucci, "Computer simulation of quench propagation in QUELL", *Adv. Cryo. Eng.*, vol. 43, pp. 181-188, 1998.
- [5] A. Martinez, "Numerical model for helium flow in a dual-channel CICC", 17-th International Cryogenic Engineering Conference (ICEC17), 14-17 July 1998, Bourmemouth, UK.
- [6] R. Zanino and L. Savoldi, "Stability modeling of ITER CS and TF CICC using the MITHRANDIR code", Politecnico di Torino Report PT DE 478/IN, April 1998.
- [7] S. DePalo, C. Marinucci, and R. Zanino, "Stability estimate for CICC with cooling channel using one- and two-fluid codes", *Adv. Cryo. Eng.*, vol. 43, pp. 333-339, 1998.
- [8] L. Bottura and A. Shaji, "Numerical quenchback in thermofluid simulations of superconducting magnets", *Int. J. Num. Methods Engng.*, in press.